CHAPTER 3

METHODOLOGY

3.1 Introduction

The first section of this chapter explains the hardware development of the CCD linear sensor system, followed by the mathematical modelling based on the CCD linear sensor system. In order to run simulations and derive a theoretical value for the data, mathematical modelling is implemented in the LabVIEW software.

3.2 Flow Chart of the Methodology

The overall methodology is concluded in the flow chart shown in Figure 3.1. The experiment starts with an analysis of the characteristics of light distribution of the ruby, followed by the hardware and software development. Then the data obtained from both simulation and experiment are compared and analyzed statistically. If the data is not sufficient (less than 15 data for each sample of experiment) or there are too many errors in the data, the data cannot be used to validate the system using statistical engineering analysis. Hence, the experiments need to be repeated. Once the satisfactory data is obtained, the relative accuracy of the data is observed.

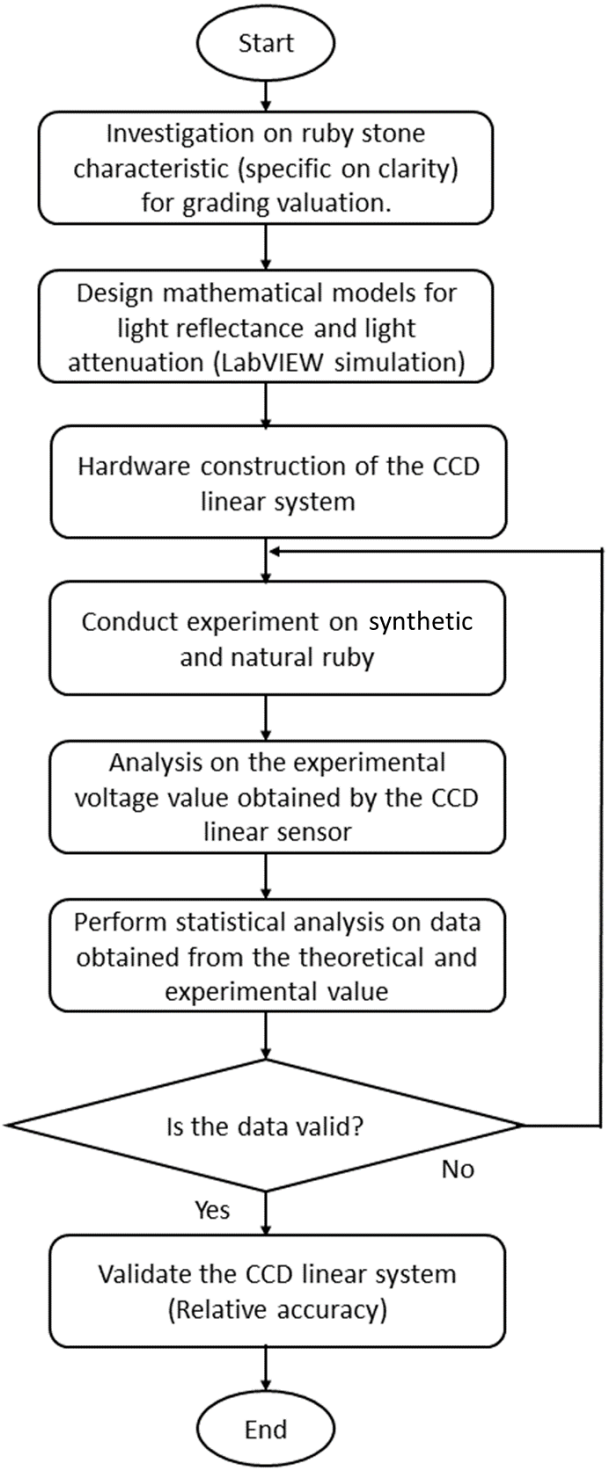

Figure 3.1 Flow Chart of the Methodology.

3.3 Mathematical Modelling on the Effects Due to Particle

The mathematical model developed to analyze the light distribution characteristic is as follows. As light passes through a translucent particle, three impacts occur: absorbance, reflectance, and dispersion (neglected due to its complex mathematical model and the fact that the particle size of interest is much greater than the wavelength of the incident light) (Idroas, 2014). The following subsection explains the mathematical modeling for light reflectance and absorption and their corresponding LabVIEW simulation (Figure 3.2). Finally, the theoretical values for the CCD sensor's voltage outputs are estimated using the refractive index of a ruby of 1.762, as stated in the GIA database (*Gemology Tools Professional*, 2016).

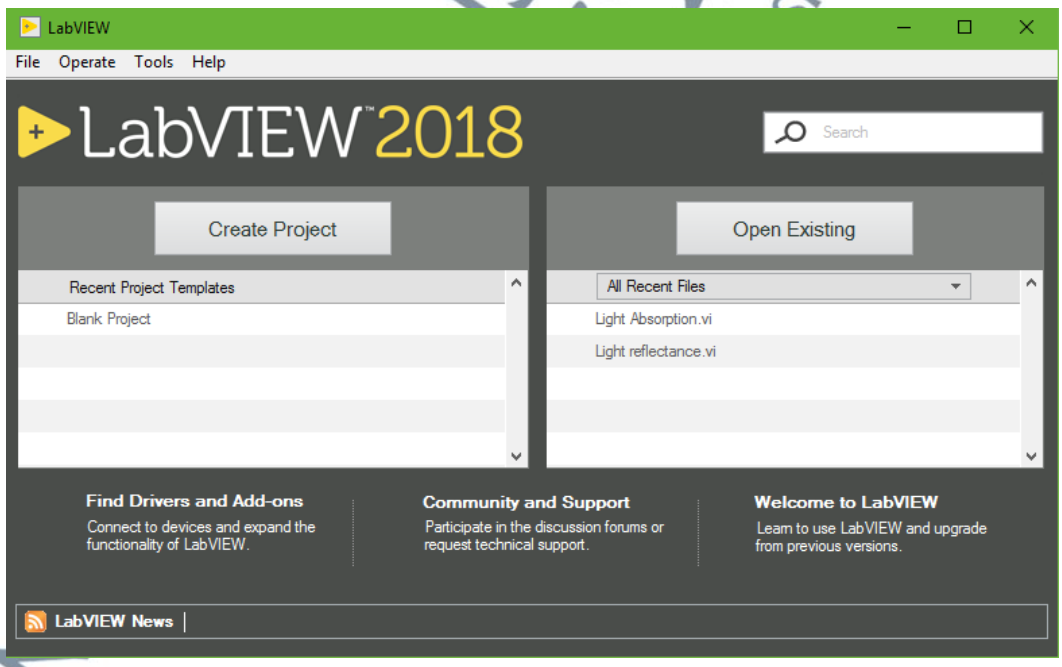

Figure 3.2 LabVIEW 2018 Software Interface.

Two conditions must be considered. The first condition is that the light is absorbed and attenuated when it enters the ruby. The other condition is that the light is reflected away as it reaches the ruby's surface. This chapter shows that the mathematical modelling is designed according to the light characteristics of the ruby, where the light travels through the air and passes through the ruby. Later in Chapter 4, these models will be applied to obtain the expected refractive index of the synthetic and natural ruby samples involved in the experiments.

3.3.1 Light Reflectance

This research involves the light traveling from the source (laser) to the ruby through the air. Light reflectance occurs when light travels from the air and hits the ruby's surface, losing energy. When light passes via a light reflection interface, energy is lost (Idroas, 2004), which in this case refers to the air–ruby interface. Reflectance (*R*) is the ratio of light reflection on the surface (Durmus et al., 2020; Idroas, 2004; Mohd Rahalim et al., 2021).

$$R = \left[\frac{(n_1 - n_2)}{(n_1 + n_2)}\right]^2 \tag{3.1}$$

n_1 is the transmitted refractive index, while n_2 is the incidence refractive index, according to Equation (3.1). *R* represents the least surface reflection from planes where the light beam is normal to the surface. As the angle of the incident beam rises, a greater amount of light is reflected (Idroas, 2014; Raisin et al., 2021). This reflection decreases

the amount of light emitted through the ruby. The final light reflectance can be obtained using Equation (3.2) where I_i is the initial light intensity (Durmus et al., 2020; Idroas, 2014).

$$I_{final\ reflectance} = I_i - \left[I_i \left(\frac{n_2 - n_1}{n_2 + n_1} \right)^2 \right] \tag{3.2}$$

The LabVIEW programming construction of the above Equation (3.2) is as in Figure 3.3.

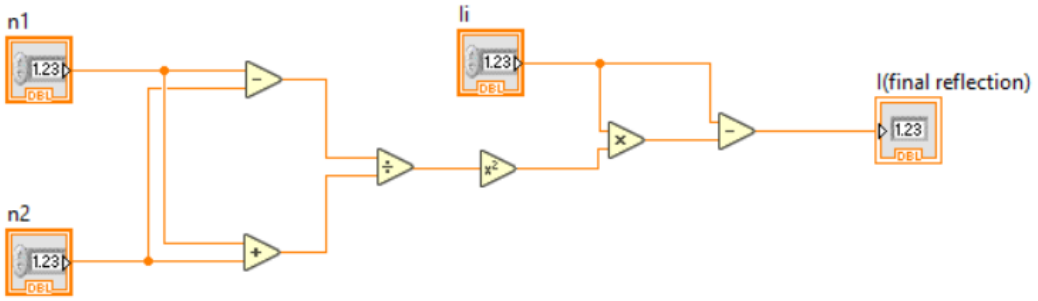

Figure 3.3 LabVIEW Programming for Light Reflectance Equation (3.2).

3.3.2 Light Attenuation

Light attenuation is the process by which light is absorbed and turned into energy when it passes through a medium. According to Beer–law, Lambert's the object density along the optical path attenuates the output light intensity exponentially (Idroas, 2014; Idroas et al., 2010). The light is absorbed by the ruby in this experiment, which

becomes the effective light that falls on the CCD linear sensor. The light attenuation is represented by the Equations (3.3) and (3.4) below:

$$I_{out} = I_{in}e^{-\alpha x} \tag{3.3}$$

$$\ln\left(\frac{I_{in}}{I_{out}}\right) = \alpha x \tag{3.4}$$

In this equation, α is the linear attenuation coefficient and x is the distance travelled by the light. α for the ruby is 0.003 mm^{-1}, and x is the diameter of the ruby which is 19.18 mm. The line integral or sum of the distribution of linear attenuation coefficients within the object is equal to the natural logarithm of the ratio of incident intensity to transmitted intensity (Durmus et al., 2020; Idroas, 2014; Raisin et al., 2021). The LabVIEW programming for the equation is shown in Figure 3.4.

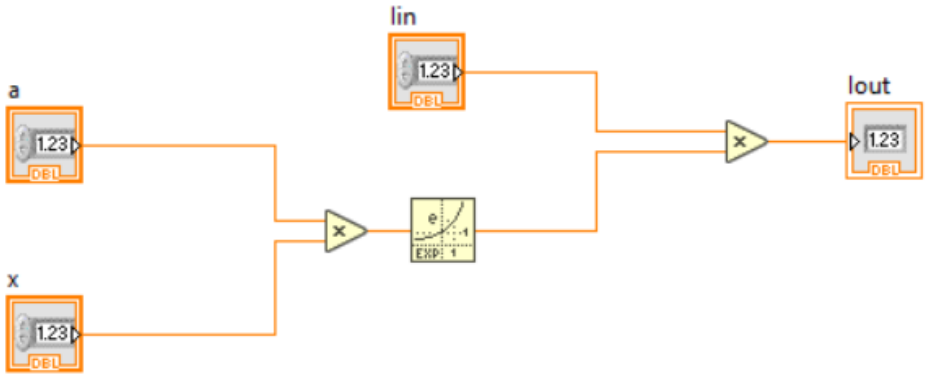

Figure 3.4 LabVIEW Programming for Light Absorption Equation.

This mathematical modelling will be applied in Chapter 4, which involves Equations (3.2) and (3.3). These two equations are used to find the expected refractive index values for the synthetic and natural rubies when investigated using the CCD linear sensor system.

3.3.3 The Mathematical Modeling Involved in the CCD Linear Sensor System

In the CCD linear sensor system, the first situation occurs when light travels from the laser toward the ruby. As this light hits the surface of the ruby, reflection occurs where the light gets reflected away from the ruby. In this situation, the calculation of the light intensity involves the light reflectance equation, which is Equation (3.2). The incidence refractive index in this situation will be the refractive index of air, which is equal to 1. The transmitted refractive index will be the refractive index of the ruby with a value of 1.76 (*Gemology Tools Professional*, 2016). Hence, the light intensity during the first situation will be calculated using Equation (3.2) as follows:

$$I_1 = I_i - \left[I_i \left(\frac{n_{ruby} + n_{air}}{n_{ruby} + n_{air}} \right)^2 \right], \tag{3.5}$$

$$I_1 = I_i - \left[I_i \left(\frac{1.76 - 1}{1.76 + 1} \right)^2 \right], \tag{3.6}$$

$$I_1 = 0.9242 I_i. \tag{3.7}$$

When the light enters the ruby, it gets absorbed. Thus, the light absorption Equation (3.3) will be used to calculate the light intensity in this second situation. The α of the ruby is 0.003 mm^{-1}, and x of the ruby is 19.18 mm. Hence, the light intensity of the ruby is determined by the following equation.

$$I_2 = I_1 e^{-(0.003\ \text{mm}-1)(19.18\ mm)}, \tag{3.8}$$

$$I_2 = 0.9242\ I_i. \tag{3.9}$$

In the third situation, the light travels out of the ruby toward the CCD linear sensor. This situation involves the reflection of light from the surface of the ruby toward the CCD linear sensor. Thus, Equation (3.2) will be used in this situation, where the transmitted refractive index is the refractive index of the air, and the incidence refractive index is the refractive index of the ruby. The calculation is performed using the following equations:

$$I_2' = I_2 - \left[I_2 \left(\frac{n_{air} - n_{ruby}}{n_{air} + n_{ruby}} \right)^2 \right], \tag{3.10}$$

$$I_2' = 0.9242 I_i - \left[0.9242 I_i \left(\frac{1 - 1.76}{1 + 1.76} \right)^2 \right], \tag{3.11}$$

$$I_2' = 0.8541 I_i. \tag{3.12}$$

As a deduction, the theoretical final light intensity ratio, $\frac{I_2'}{I_i}$, in the laser ON situation with the presence of the ruby is 0.8541. In the laser OFF condition, the

luminescence light from the ruby is reflected toward the CCD linear sensor. Hence, only the light reflectance Equation (3.3) is used to calculate the light intensity. The calculation is as follows:

$$I'_{2laserOFF} = I_i - \left[I_i \left(\frac{1 - 1.76}{1 + 1.76} \right)^2 \right], \tag{3.13}$$

$$I'_{2laserOFF} = 0.9242 I_i. \tag{3.14}$$

Thus, the final light intensity ratio, $\frac{I'_{2laserOFF}}{I_i}$, of this case is 0.9242.

3.4 Hardware Development of CCD Linear Sensor System

The CCD linear sensor system hardware comprises a black box, laser, CCD, and objects that need to be evaluated. A laser is a monochromatic, consistent beam of light with low distortion, low noise, and an extremely directional beam that can travel long distances at a low divergent angle. There are two kinds of laser diodes: low-power lasers and high-power lasers. The high-power laser, optically saturates the CCD sensors and raises their temperatures (Idroas et al., 2011; Jamaludin, 2016).

Jamaludin (2016) conducted a study on the optical tomography system using the CCD linear sensor. The authors proposed an approach to detect solid objects in crystal-clear water using the CCD linear sensor. This research will use the CCD linear sensor

to detect the light intensity of the ruby, but the light will travel through the air instead of crystal-clear water.

The Sony ILX551A CCD linear sensor is in this system owing to its better advantages compared to the other types of CCDs, as stated in Section 2.4.1. Figure 3.5 displays the CCD linear sensor Sony ILX551A spectral sensitivity features. The high relative sensitivity of Sony ILX551A sensor, marked by the horizontal dashed line, was believed to be greater than 0.85. The effective spectrum of light for the CCD linear sensor Sony ILX551A lies between the wavelength of 430 nm and 680 nm as marked by the vertical dashed lines (Jamaludin, 2016; Sony Corporation, n.d.).

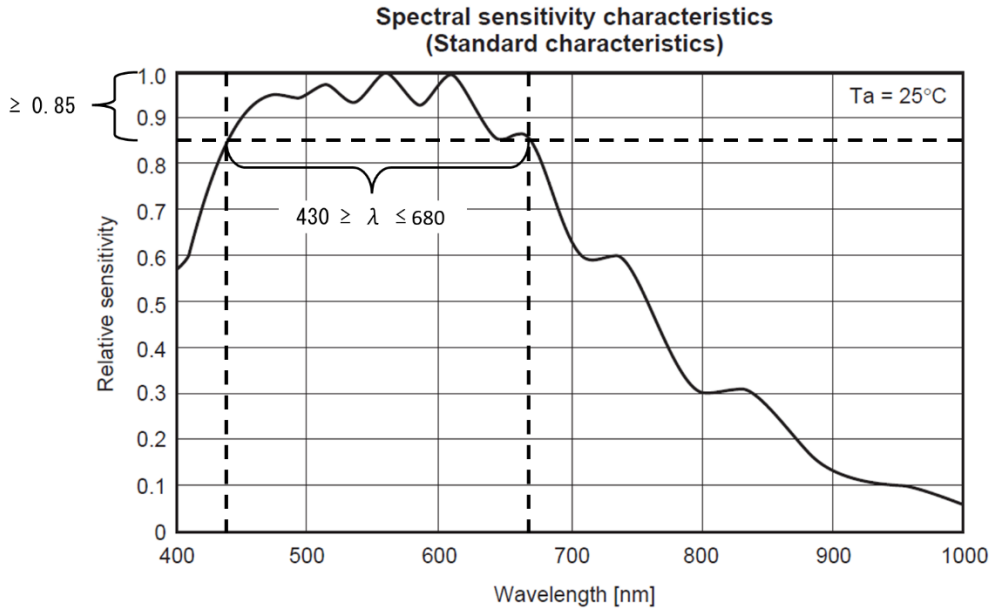

Source: Sony Corporation (n.d.)

Figure 3.5 Spectral Sensitivity Characteristic Chart of Sony ILX551A CCD Linear Sensor.

The overall system of the CCD is illustrated in Figure 3.6. The CCD linear sensor system is designed in a black opaque box to provide minimum external light possible where the laser is beamed toward the CCD linear sensor. A black opaque box is used to improve the accuracy of the CCD sensor, allowing the CCD to receive the most intensity of light from the ruby with the fewest external light sources. Figure 3.6 illustrates the front view of the CCD linear sensor system. The ruby gemstone with the diameter of 19.18 mm is placed between the laser and CCD linear sensor. A light filter is placed in between the laser and the ruby to reduce the noise in the light intensity data as explained in the Chapter 4.

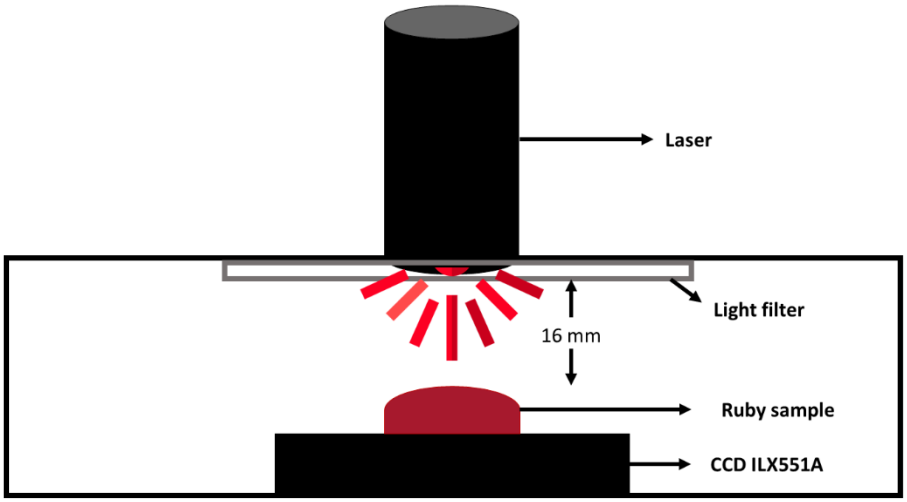

Figure 3.6 Illustration of the CCD Linear System Setup.

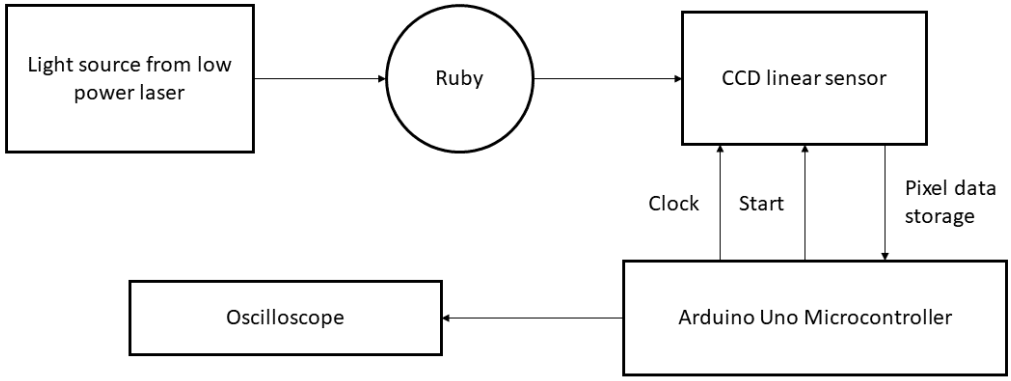

Figure 3.7 Block Diagram of the CCD Linear Sensor System.

Figure 3.7 depicts the block diagram of the CCD linear sensor system. The light from the ruby falls onto the CCD linear sensor as the laser is directed toward it and then the laser light passes through it. The light received is subsequently analyzed by the CCD sensor, which turns the measured light intensity into a voltage. The Arduino Uno Microcontroller produces the clock and ROG signals required by the CCD linear sensor system. The final voltage value data is then measured using the Agilent U1620A oscilloscope.

Figure 3.8 shows the CCD linear sensor system that is connected to the resistors, capacitors and diode accordingly based on the application circuit of CCD ILX551A shown in Figure 3.9 that is obtained from the datasheet. Figure 3.10 shows the experimental setup of the CCD linear sensor system before placing it in the black opaque box, where the CCD linear sensor Sony ILX551A is connected to the Arduino Uno Microcontroller and the oscilloscope. A laser is beamed towards the ruby stone and the light that passes through the ruby is captured by the CCD linear sensor as shown

in Figure 3.10. The front view of the CCD linear sensor system experimental setup is depicted in Figure 3.11.

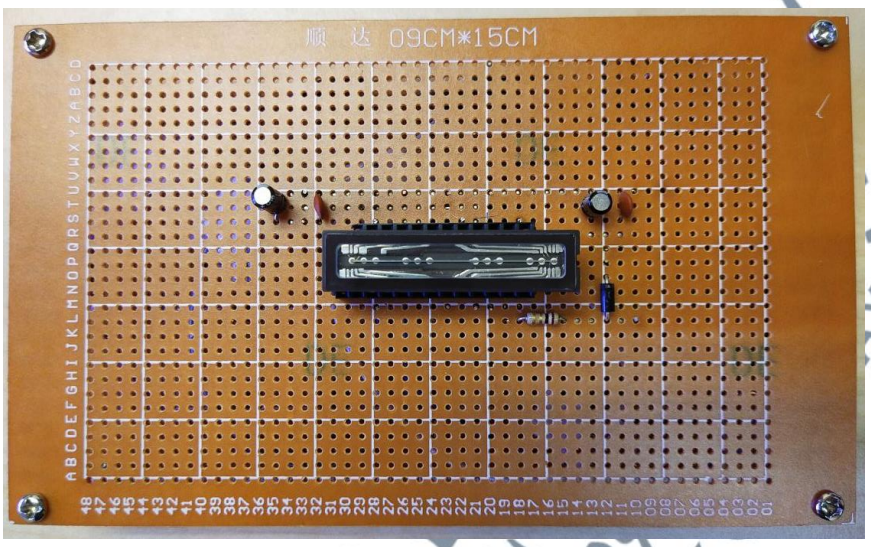

Figure 3.8 The Hardware Development of CCD Linear Sensor System.

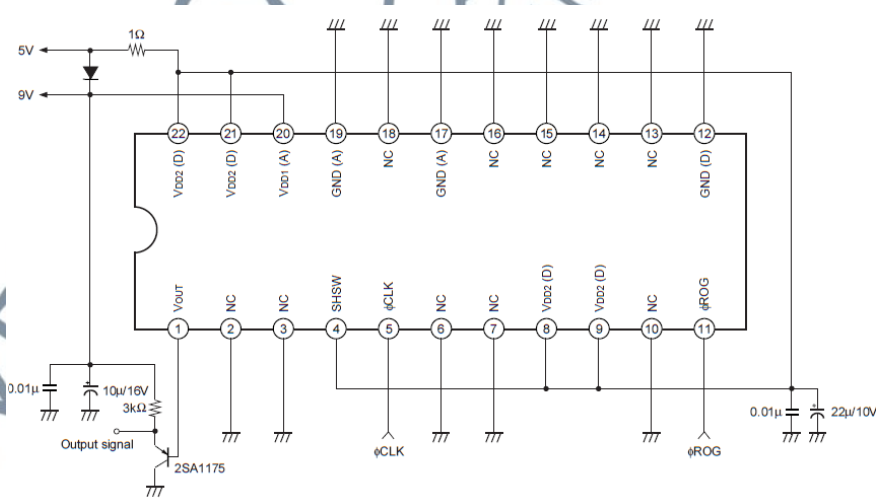

Source: Sony Corporation (n.d.)

Figure 3.9 Application Circuit of CCD ILX551A.

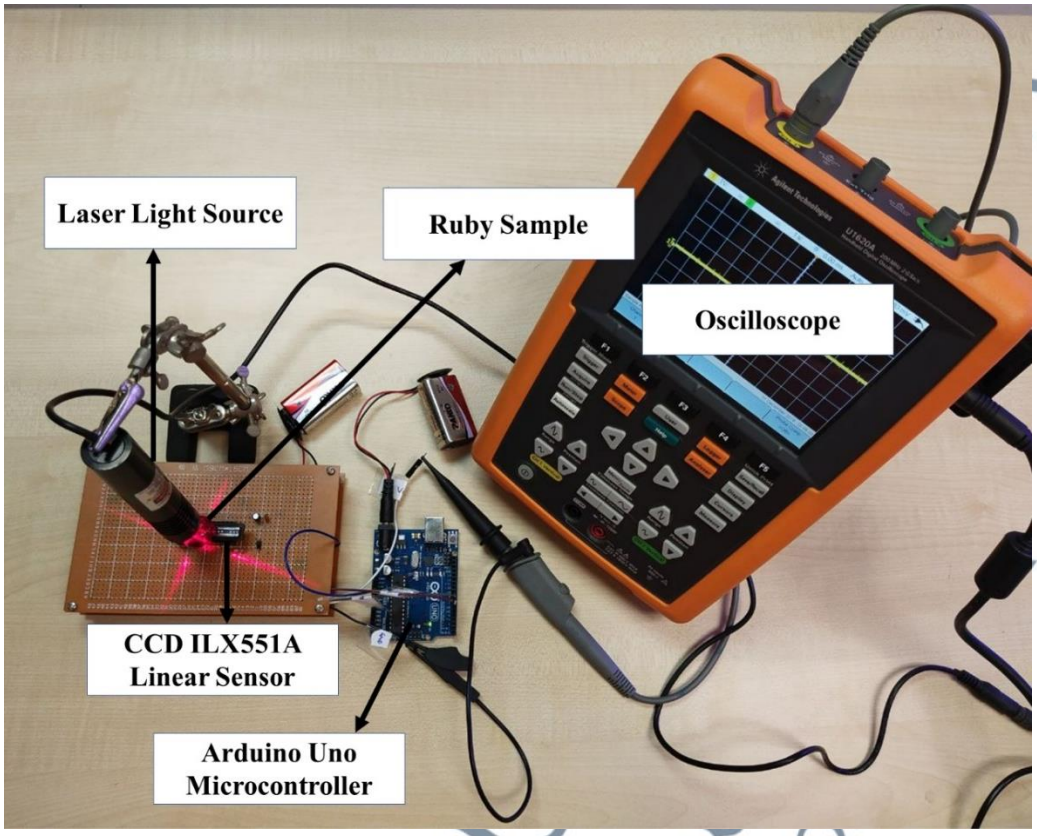

Figure 3.10 Experimental Setup of the CCD Linear Sensor System.

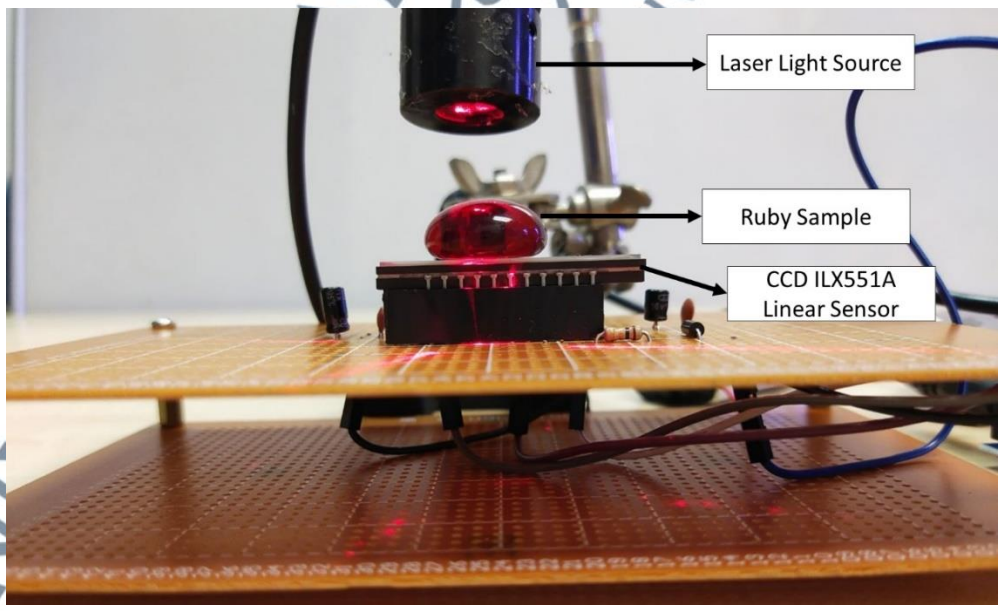

Figure 3.11 Front View of the CCD ILX551A Linear Sensor System Experimental Setup.

The CCD linear sensor system is then placed in a black opaque box as shown in Figure 3.12. A light filter is placed at the opening of the box that is in between the laser and the ruby. The light intensity in the black box is maintained at 0.5 lux to avoid saturation of the CCD linear sensor as shown in Figure 3.13 Then, the completed CCD linear system circuit is connected to the oscilloscope and the Arduino Uno Microcontroller, where the ATMEGA328P microcontroller is programmed using the codes in Figure 3.14 to run the clock signal that will trigger the light intensity data from the CCD linear sensor.

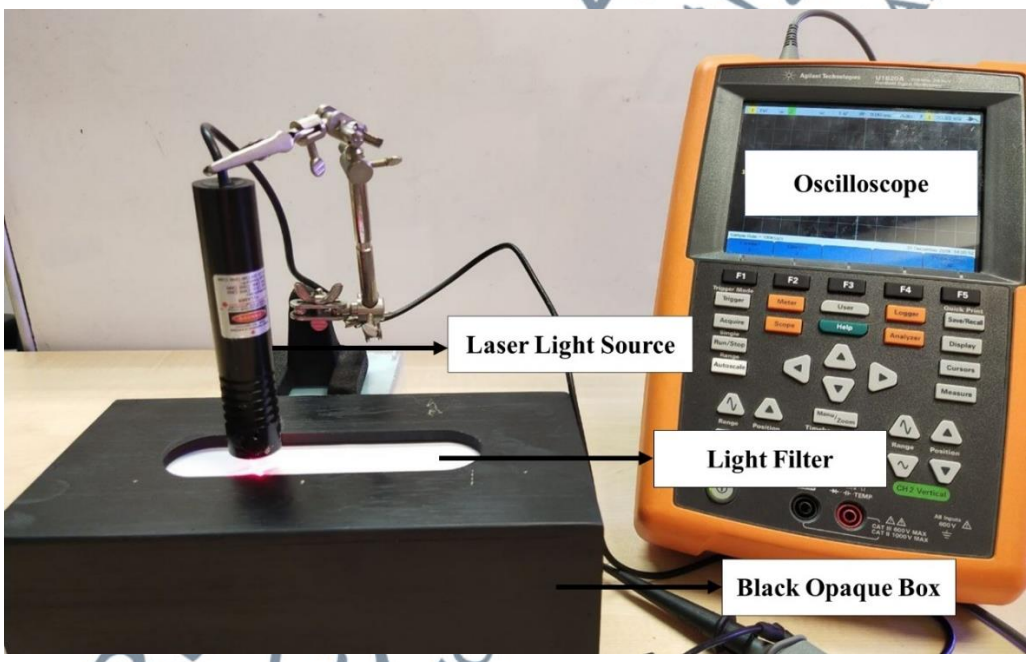

Figure 3.12 Experimental CCD ILX551A Linear Sensor Setup in a Black Opaque Box.

Figure 3.13 A Luxmeter Showing the Light Intensity Inside the Black Opaque Box.

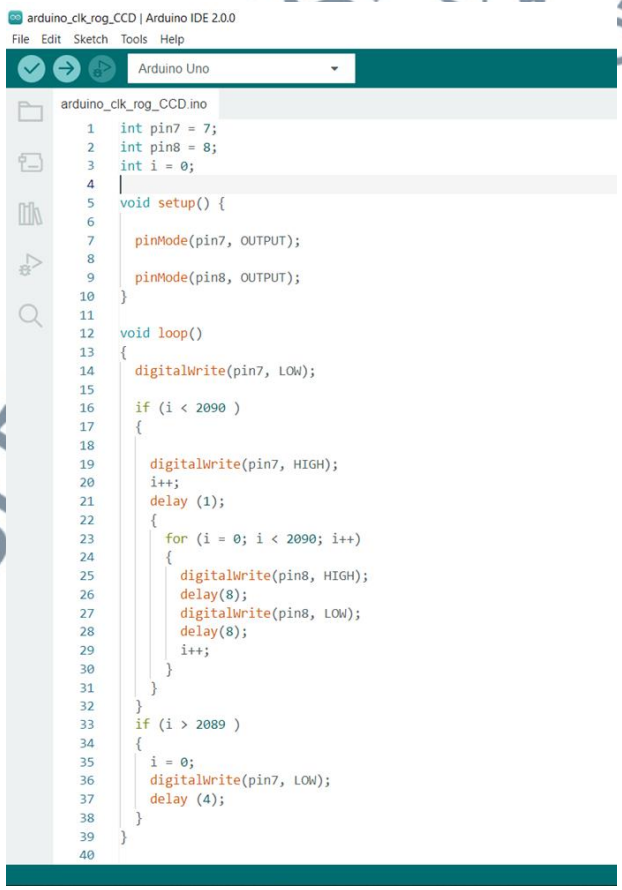

Figure 3.14 Arduino Codes for CCD Sony ILX551A.

The Sony ILX551A CCD sensor requires two input signals, the readout gate (ROG) and clock signals, therefore both signals must be programmed. The signals are programmed in C++ language in the Arduino Integrated Development Environment software. The program is then uploaded into the programmable integrated circuit (ATMEGA328P-PU). In particular, the CCD Sony ILX551A sensor has 2048 sensitive pixels. According to the datasheet, there are 2090 pixels. Consequently, 2090 clock signals are programmed. Other than the 2048 sensitive pixels, the remaining pixels act as the dummy signal at the start and end of each clock signal. The programming code script is shown in Figure 3.14.

Before uploading the programmed codes into the Arduino board, the codes are run in the Proteus software for verification. Based on the datasheet of the CCD sensor system, it should have two main signals—the clock and ROG signals—that triggers the clock signal (Figure 3.9). The codes are uploaded to the Arduino Uno board in the Proteus, and the waveforms for the clock and ROG signals are observed through the virtual oscilloscope, as shown in Figure 3.15. In Figure 3.15, it can be observed in the digital oscilloscope that the ROG signal (blue line) successfully triggers the end of the period for the clock signal (yellow line). One complete period has a 2090 clock cycle that includes 2048 effective signals and the rest as dummy signals programmed in the Arduino.

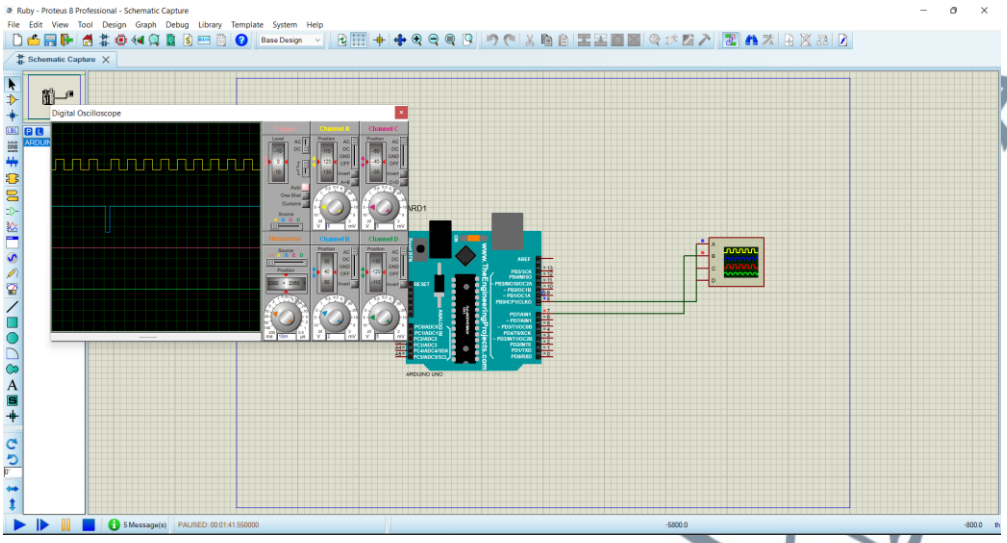

Figure 3.15 Simulation of the CCD Linear Sensor System Codes in Proteus.

Figure 3.16 illustrates the flow chart of the program. The program starts with declaring the variable pin7 and pin 8 where both are the ROG output pin and clock output pin respectively. Then, initialize the counter *i* = 0. The pin7 and pin8 also initialize at 0 value. Then, the loop starts whereby when the counter *i* less than 2090, the pin7 will give the high value of 1 and the pin8 will alternately executes low and high value with the delay of 8us in between each cycle. When the counter becomes more than 2089 it means that one set of data have been executed, the counter will be set to 0 and pin7 also set to low value. Then, the next set of data will be continuously executed following the same execution steps as above.

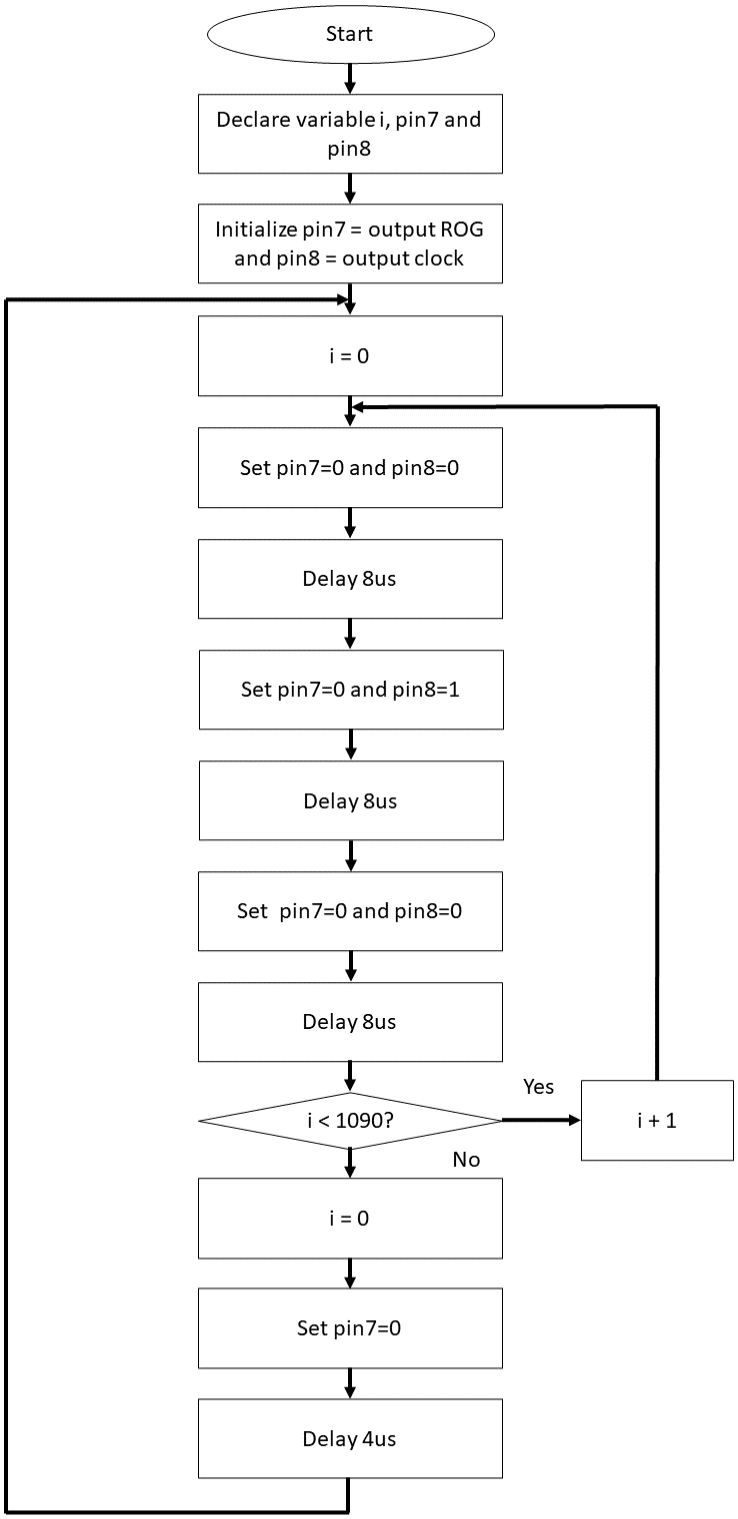

Figure 3.16 Flow Chart of the Clock (Pin8) Signal and ROG (Pin7) Signal of the CCD Sony ILX551A.

The Arduino Uno Microcontroller also connects the CCD linear sensor to the Agilent U1620A oscilloscope, where the real-time signal of the light intensity acquired by the CCD linear sensor is collected. The Agilent U1620A oscilloscope used for this step is shown in Figure 3.17. The data collected from the oscilloscope is in the form of a voltage that represents the light intensity captured by the CCD linear sensor.

Figure 3.17 Agilent U1620A Oscilloscope Used to Produce the Digital Signal from the CCD Linear Sensor System.

When a ruby is placed in the CCD linear sensor system, the signal appearing on the oscilloscope is retrieved and the data distribution of the CCD voltage output is plotted as shown in Figure 3.18. This experiment is conducted using the CCD linear

sensor to detect the transparency of the ruby, which is directly related to the light intensity of the ruby. The CCD linear sensor detects the light intensity and convert it into the voltage value. Since this CCD linear sensor is very sensitive to light, each pixel captured can detect each slightest change that occurs in the system.

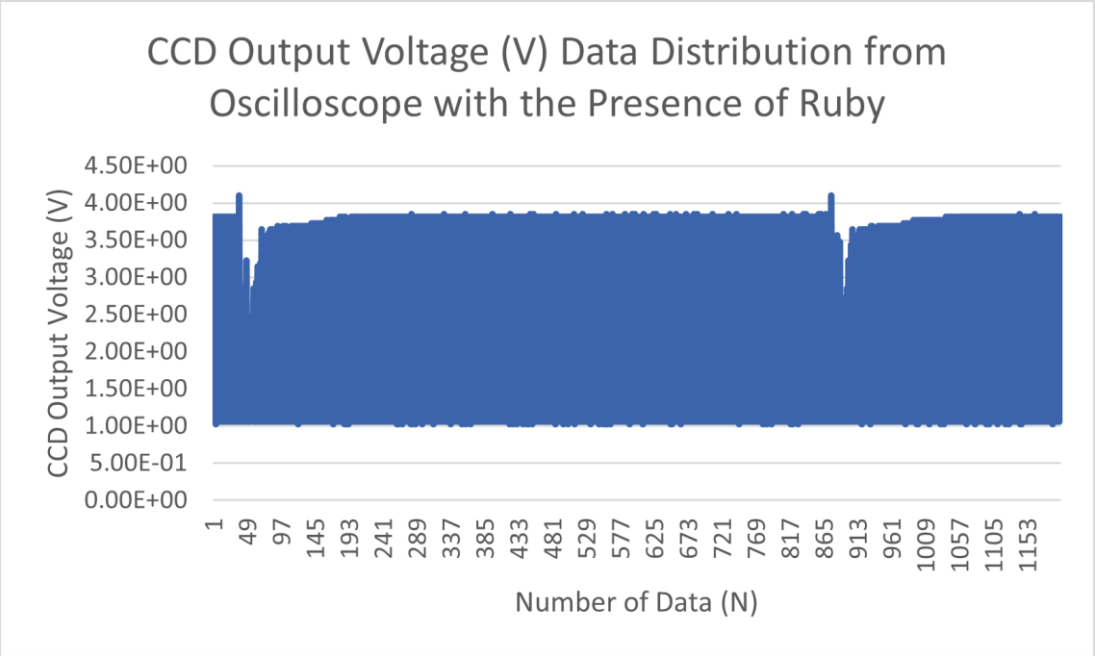

Figure 3.18 Data Distribution of the CCD Voltage Output from the Oscilloscope when Ruby Appears in the System.

Essentially, a suitable environment is prepared to prevent the CCD linear sensor from being saturated. The CCD linear sensor requires relative humidity to be within 65%–85% and the temperature to be within 25ºC–33ºC (Jamaludin et al., 2017, 2018). Similarly, the laser is maintained at 0.5 lux for optimum CCD linear sensor working

conditions (Jamaludin, 2016). Figure 3.19 shows a synthetic ruby sample (man-made red silica glass), and Figure 3.20 shows a natural ruby stone from Myanmar.

Figure 3.19 Synthetic Ruby Stone (Man-Made Red Silica Glass).

Figure 3.20 Natural Ruby Stone from Myanmar.

3.5 Laser Diode System

A laser diode is used in the CCD linear sensor system as it helps in producing effective results. Although the ruby itself can radiate and produce its own fluorescence when placed under natural or artificial light, the CCD linear sensor system cannot effectively detect the light from the ruby because the CCD linear sensor is very sensitive to light. Thus, only the light solely from the ruby is needs to be detected. Additionally, the CCD linear sensor system is designed in a black opaque box to ensure minimum intervention from lights of any other possible sources invading the CCD linear sensor system. Because the CCD linear sensor system runs in an almost completely dark environment, the laser diode is needed to help the ruby radiate and effectively show its light characteristics on the CCD linear sensor. In this experiment, a red laser diode with a 630 nm to 650 nm wavelength is used (Jamaludin, 2016). The laser diode is displayed in Figure 3.21.

Figure 3.21 Red Laser Diode with 650nm Wavelength.

3.6 Summary

In this chapter, there are three main sections. First, the discussion on the mathematical modelling which involves the light reflection and light absorption equation. Both of these equations are synthesized according to the situation in the laser condition ON and OFF and the final light intensity equation for both conditions are executed. The following subsection provides detail explanation on the hardware development of the CCD linear sensor system. Lastly, brief explanation on the laser diode system is provided in the last section.

The next chapter presents the experiments conducted using the CCD linear sensor system. The results and discussions for each experiment are explained briefly and the results are validated using the statistical analysis method. The accuracy of the CCD linear sensor system is also calculated in Chapter 4.